

Non-Standard Neutrino Interactions : Obviating Oscillation Experiments

Debajyoti Choudhury¹, Kirtiman Ghosh² and Saurabh Niyogi³

¹*Department of Physics and Astrophysics, University of Delhi, Delhi 110007, India*

²*Institute of Physics, Bhubaneswar 751005 & HBNI, Mumbai, India*

³*Department of Physics, Gokhale Memorial Girls' College, Harish Mukherjee Road, Kolkata 700020, India **

Searching for non-standard neutrino interactions, as a means for discovering physics beyond the Standard Model, has one of the key goals of dedicated neutrino experiments, current and future. We demonstrate here that much of the parameter space accessible to such experiments is already ruled out by the RUN II data of the Large Hadron Collider experiment.

Precision measurements of the neutrino mixing parameters, made over the past few decades has significantly shortened the list of unanswered questions in the standard scenario to just the issues of the neutrino mass hierarchy i.e., $\text{sign}(\delta m_{31}^2)$, the CP phase and the correct octant for the mixing angle θ_{23} . While the simplest way to generate neutrino masses is to add right handed neutrino fields to the Standard Model (SM) particle content, it is hard to explain their extreme smallness. Several scenarios going beyond the SM have been proposed to this end, often tying up with other unanswered questions such as (electroweak) leptogenesis [1, 2], neutrino magnetic moments [3–6], neutrino condensate as dark energy [7, 8]. An agnostic alternative is to add dimension-five terms consistent with the symmetries and particle content of the SM, which naturally leads to desired tiny Majorana masses for the left-handed neutrinos. Irrespective of the approach, once new physics is invoked to explain the non-zero neutrino masses, it is unnatural to exclude the possibility of non-standard interactions (NSI) as well. Indeed, NSI has been studied in the context of atmospheric neutrinos [9–14], CPT violation [15, 16], violation of the equivalence principle [13], large extra dimension models [17], sterile neutrinos [18–20] and collider experiments [21–24].

At sufficiently low energies, a wide class of new physics scenarios can be parameterised, in a model independent way, through the use of effective four-fermion interaction terms. While these, in general, would incorporate both charged-current (CC) and neutral-current (NC) interactions, we shall confine ourselves largely to the latter (coming back to the former only later). The dimension-6 neutrino-quark interactions can, then, be expressed, in terms of the chirality projection operators P_X ($X = L, R$), as

$$\mathcal{L}_4 = -2\sqrt{2} G_F \epsilon_{\alpha\beta}^{qX} (\bar{q}\gamma_\mu P_X q) (\bar{\nu}_\alpha \gamma^\mu P_L \nu_\beta) + H.c., \quad (1)$$

where α, β denote the neutrino flavours, q is a quark field, and $\epsilon_{\alpha\beta}^{qX}$ are arbitrary constants, presumably $\lesssim \mathcal{O}(10^{-2})$. It should be noted that flavour-changing currents are allowed at the neutrino-end but not for the quarks, with

this restriction being imposed to evade the strong bounds from decays such as $K \rightarrow \pi \nu \bar{\nu}$ or $B \rightarrow K \nu \bar{\nu}$. While this might seem an unnatural choice (note also that analogous currents involving the charged leptons would, typically, be subjected to even stronger constraints), the inclusion of such flavour-changing neutrino currents is not crucial to the main import of this paper.

Neutrino oscillation experiments can probe such NSI by exploiting the interference with the SM amplitude, with the NC interactions altering the refractive index, as evinced by the far detectors. The excellent agreement of data with the standard flavour conversion paradigm implies that reasonably strong constraints are already in place with these slated to improve considerably in the next-generation experiments.

At the LHC, operators as in eq.(1) would lead to a change in the rates for final states comprising a hard jet and missing energy. For $q = u, d$, this would be dominated by parton-level processes such as $q + g \rightarrow q + \nu + \bar{\nu}$ and $q + \bar{q} \rightarrow g + \nu + \bar{\nu}$. With the (anti-)neutrinos going undetected, different choices of α, β would lead to essentially the same observables, and are, hence, indistinguishable from each other. While the aforementioned subprocesses dominate at the partonic level, the detector could also register multiple jets (with missing energy) accruing from initial and final state radiations, hadronization etc. Indeed, such processes have been studied extensively [25–28] as a search tool for new physics scenarios such as supersymmetry, extra dimensions as well as generic Dark Matter models.

To generate events at the LHC, we have incorporated the 4-fermi operators (of eq.(1)) in FeynRules (v2.3.13) [29, 30] to generate model files for MadGraph5_aMC@NLO (v2.2.1) [31]. In order to compute the cross sections, we have used the NNPDF23lo1 parton distributions [32] with the factorization and renormalization scales kept fixed at the central m_T^2 scale after k_T -clustering of the event. Initial and final state radiation, showering and hadronization were simulated with PYTHIA 6.4 [33]. The reconstruction of physics objects (jets, leptons, \cancel{E}_T etc.) was done in accordance with the prescription of the ATLAS monojet + \cancel{E}_T analysis [26]. We have used FastJet [34] and the anti- k_T jet clustering algorithm [35] with a radius parameter of 0.4 for jet reconstruction. While only jets with $p_T > 20$ GeV and $|\eta| < 2.8$ are retained, electron (muon) candidates are

* ¹debajyoti.choudhury@gmail.com

²kirti.gh@gmail.com

³saurabhphys@gmail.com

required to have $p_T > 20$ (10) GeV and $|\eta| < 2.47$ (2.5). The discarding any putative jet lying within a distance $\Delta R = \sqrt{\Delta\eta^2 + \Delta\phi^2} < 0.2$ (0.4) of an electron (muon) candidate resolves overlaps. Moreover, for events with $0.2 < \Delta R_{ej} < 0.4$, the electron is removed as it is likely to have emanated from a semileptonic b-hadron decay. The missing transverse momentum is reconstructed using all energy deposits in the calorimeter (including unassociated calorimeter clusters) up to pseudorapidity $|\eta| < 4.9$. Only events with zero leptons, $\cancel{E}_T > 250$ GeV and at least one jet (satisfying the aforementioned preselection criteria) are selected for further analysis.

A monojet-like final state topology demands a leading jet with $p_T > 250$ GeV and $|\eta| < 2.4$. On the other hand, a maximum of four jets with $p_T > 30$ GeV and $|\eta| < 2.8$ are allowed. Additionally, to reduce the multijet background contribution where a large \cancel{E}_T can originate from jet energy mismeasurement, each of the jets must satisfy a azimuthal separation criterion of $\Delta\phi(\text{jet}, \vec{\cancel{E}}_T) > 0.4$. Subsequently, different signal regions (IM1–SR10) are defined, in accordance with the ATLAS monojet-like selection criteria [26], with progressively increasing thresholds for \cancel{E}_T . These are summarized in Table I.

SR	\cancel{E}_T (GeV)	σ_{obs}^{95} (fb)	σ_{exp}^{95} (fb)	
		36.1 fb^{-1}	100 fb^{-1}	300 fb^{-1}
IM1	> 250	531	160^{+80}_{-43}	80^{+41}_{-31}
IM2	> 300	330	94^{+48}_{-37}	47^{+24}_{-18}
IM3	> 350	188	52^{+26}_{-21}	26^{+13}_{-10}
IM4	> 400	93	28^{+13}_{-11}	14^{+7}_{-5}
IM5	> 500	43	10^{+5}_{-4}	$5.1^{+2.4}_{-1.9}$
IM6	> 600	19	$4.8^{+2.2}_{-1.8}$	$2.5^{+1.1}_{-0.9}$
IM7	> 700	7.7	$2.9^{+1.3}_{-1.0}$	$1.5^{+0.6}_{-0.5}$
IM8	> 800	4.9	$1.8^{+0.8}_{-0.6}$	$0.9^{+0.4}_{-0.3}$
IM9	> 900	2.2	$1.2^{+0.5}_{-0.4}$	$0.6^{+0.3}_{-0.2}$
IM10	> 1000	1.6	$0.8^{+0.3}_{-0.3}$	$0.4^{+0.2}_{-0.1}$

TABLE I. The different monojet-like signal regions as defined by the ATLAS collaboration [25, 26], and their corresponding 95% CL upper limits (for 36.1 fb^{-1} data) on the cross section (σ_{obs}^{95}) due to all BSM effects. Assuming that the agreement between the data and SM would persist, σ_{exp}^{95} represent the expected 95% CL upper limits for integrated luminosities of 100 and 300 fb^{-1} .

For each of these signal regions, ATLAS collaboration [25, 26] have measured the cross sections with 36.1 fb^{-1} data of 13TeV LHC and provided 95% CL upper limits (σ_{obs}^{95} , also shown in Table I) on the contributions from generic NP scenarios. In the present context, these could be translated to ellipsoids in the ϵ -space. Limiting ourselves to a single pair of operators (we restrict ourselves to $q = u, d$) at a time, the NSI contributions (denoted by σ_{BSM}) corresponding to the signal region IM9 is illustrated in Fig.1.

The excellent agreement between the numbers of

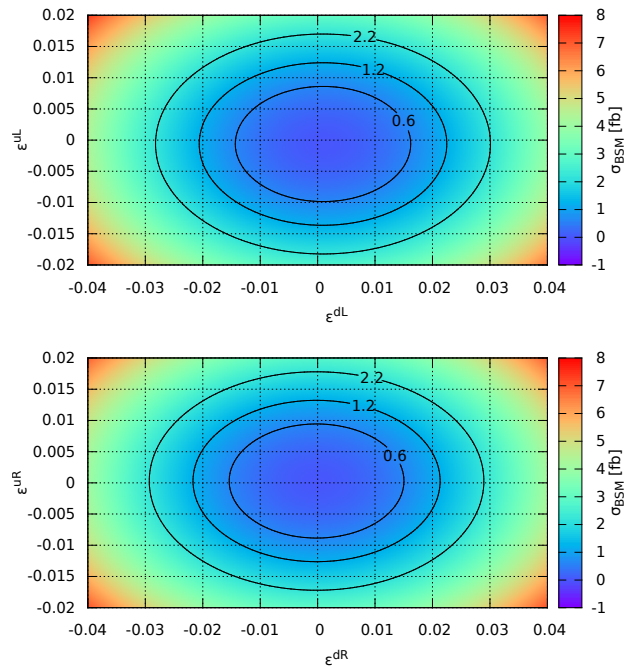


FIG. 1. NSI contributions (shown by color gradient) to the ATLAS search regions for monojet+ p_T signature in SR-IM9 as a function of ϵ^{uL} and ϵ^{dL} (upper panel) and ϵ^{uR} and ϵ^{dR} (lower panel).

events observed by the ATLAS detector and that expected within the SM can be used to impose limits on the parameters $\epsilon_{\alpha\beta}^{qX}$. As pointed out earlier, the final state is independent of the neutrino flavours, and indeed receives (incoherently adding) contributions from all possible flavour combinations. The ensuing constraint, can be parametrized as

$$\sum_{\alpha\beta} \sum_X \left[a_u^{-2} (\epsilon_{\alpha\beta}^{uX} - \epsilon_u^X)^2 + a_d^{-2} (\epsilon_{\alpha\beta}^{dX} - \epsilon_d^X)^2 \right] < 1, \quad (2)$$

where the central values ϵ_q^X are as in Table II. It should be noted that, for off-diagonal couplings, $\epsilon_q^X = \text{identically}$. That $a_u < a_d$ for each case can be understood as a consequence of the larger densities for the u -quark. Similarly, the fact that $a_{u,d}$ are independent of the chirality is but reflective of the fact that, in the limit of vanishing quark masses, terms proportional to ϵ^2 are independent of chirality. The terms linear in $\epsilon_{\alpha\beta}^{qX}$ are consequences of interference with the SM amplitude, signs being indicative of constructive or destructive nature. The interferences are large for the left-chiral quarks because of their enhanced coupling with the Z -boson. In fact, for the d_L , the interference is as significant as 50% ($\sigma_{\text{int}}^{qX} / \sigma_{\text{BSM}}^{qX} = 2\epsilon_q^X (\epsilon_{\alpha\beta}^{qX} - 2\epsilon_q^X)^{-1}$) for SR-IM1 in the region ($\epsilon_{\alpha\beta}^{dL} \sim 0.02$) sensitive to LHC run-II data. However, demanding harder cuts on \cancel{E}_T reduce the interference contribution significantly. Note that not much should be read into the nonzero central values ϵ_q^X as these are

attributable to small statistical fluctuations in the data.

SRs	ϵ_u^L	ϵ_u^R	ϵ_d^L	ϵ_d^R	Observed		Expected			
					36.1 fb ⁻¹		100 fb ⁻¹		300 fb ⁻¹	
					a_u	a_d	a_u	a_d	a_u	a_d
IM1	-23	11	33	-6	564	823	311 ₄₄ ⁶⁹	453 ₆₅ ¹⁰⁰	221 ₄₇ ⁵⁰	323 ₆₈ ⁷²
IM2	-20	9	28	-5	488	716	261 ₅₇ ⁵⁹	384 ₈₄ ⁸⁷	186 ₃₉ ⁴²	273 ₅₇ ⁹¹
IM3	-17	8	24	-5	416	616	220 ₄₉ ⁴⁹	325 ₇₃ ⁷²	156 ₃₂ ³⁴	231 ₄₈ ⁵¹
IM4	-15	8	21	-4	334	499	184 ₄₀ ³⁸	275 ₅₉ ⁵⁷	131 ₂₅ ²⁹	195 ₃₈ ⁴²
IM5	-12	7	16	-3	294	451	142 ₃₂ ³⁷	219 ₄₉ ⁵⁷	103 ₂₁ ²¹	157 ₃₂ ³³
IM6	-10	5	14	-3	253	397	128 ₂₆ ²⁶	201 ₄₁ ⁴¹	92 ₁₈ ¹⁸	145 ₂₈ ²⁹
IM7	-8	4	12	-2	207	329	128 ₂₄ ²⁶	202 ₃₈ ⁴¹	92 ₁₇ ¹⁷	146 ₂₆ ²⁶
IM8	-7	3	10	-2	209	340	127 ₂₃ ²⁶	206 ₃₈ ⁴¹	90 ₁₆ ¹⁸	146 ₂₆ ²⁹
IM9	-6	3	9	-2	176	292	130 ₂₄ ²⁵	215 ₃₉ ⁴¹	92 ₁₇ ²¹	153 ₂₈ ³⁴
IM10	-5	3	8	-2	187	313	133 ₂₈ ²³	221 ₄₆ ³⁸	94 ₁₂ ²¹	157 ₂₀ ³⁵

TABLE II. The values of the parameters (each scaled up by a factor of 10^4) as in eq.(2). Also shown are the expected sizes of the ellipses assuming that the agreement of the data with the SM persists with higher luminosities.

We also show, in Table II how $a_{u,d}$ would scale with luminosity if the present level of agreement between the data and the SM expectations were to continue. A crucial component in making this comparison are the systematic uncertainties in the background estimation. Listed in Ref.[26], the dominant contributions to the uncertainty in the mono-jet background estimation arise from (i) the uncertainties in the absolute jet and missing transverse energy scales, (ii) those related to jet quality requirements, the description of the pileup, b-tagging, lepton identification and reconstruction efficiency, (iii) those in the modelling of parton-showers and choice of PDFs, and finally (iv) the lack of higher-order parton level calculations or the implementation thereof in the MC event generators. With increasing amount of data, and hence, a better understanding of the detector responses, the experimental uncertainties in the estimation of the SM backgrounds are expected to be reduced significantly. As an example, the systematic uncertainty in the background estimation in Ref.[26] has reduced nearly by a factor of 2 when compared to an earlier identical analysis [36] performed with only 3.2 fb^{-1} of data. In this even, the indicative projections of Table II assume that the experimental systematic uncertainty would be reduced by a factor of 2 (4) with accumulated luminosity of 100(300) fb^{-1} .

It is worthwhile to note that while strengthening the requirement on \cancel{E}_T increases the sensitivity (a reflection of the higher-dimensional nature of the terms), this flattens out at $\cancel{E}_T \gtrsim 600$ GeV with the SRs IM6–10 being almost equally efficient. And in the high- \cancel{E}_T region, with the semi-axes $a_{u,d}$ being much larger than ϵ_q^X , it is the former that essentially determine the shape and size of the constraint ellipsoids (or, ellipses, when projected to

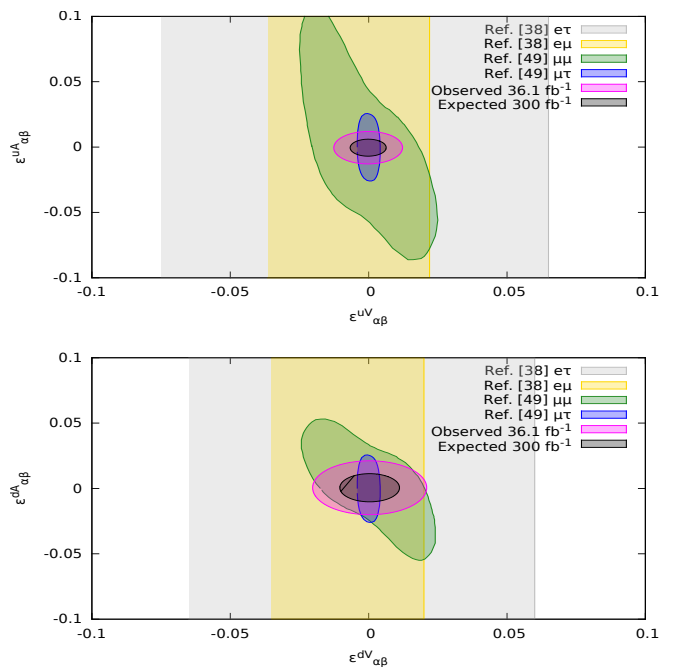


FIG. 2. Allowed parts of $\epsilon_{\alpha\beta}^{qV}-\epsilon_{\alpha\beta}^{qA}$ planes, with $q = u(d)$ in the upper(lower) panels. The bounds from neutrino experiments are flavour specific and at 90% CL, while those from the ATLAS (36 fb^{-1} at $\sqrt{s} = 13 \text{ TeV}$) apply to all flavour combinations, and at 95% CL.

a plane).

In Fig.2, we present a comparison of our bounds with those emanating from other experiments. For neutrino scattering (whether forward or otherwise) off nonrelativistic nuclei, vector quark currents contribute more than axial ones, and neutrino oscillation experiments are only sensitive to ϵ^V . Choosing to work in this basis, 90% CL bounds on $\epsilon_{e\mu}^{fV}$ and $\epsilon_{e\tau}^{fV}$ result from a global analysis [37, 38] of data from solar, atmospheric (Super-Kamiokande [39]), long-baseline accelerator experiments (MINOS [40, 41], T2K [42, 43] and reactor experiments (KamLAND [44], CHOOZ [45], Palo Verde [46], Daya Bay [47], Reno [48]). The bounds on $\epsilon_{\mu\mu}^{fV}$ and $\epsilon_{\mu\tau}^{fV}$ corresponds to the global analysis [49] of NuTeV [50] CHARM [51], CDHS [52] and atmospheric neutrino oscillation data. Note that oscillation experiments are sensitive only to off-diagonal ϵ 's and to differences between the diagonal terms (for instance, $\epsilon_{ee} - \epsilon_{\mu\mu}$ and $\epsilon_{\tau\tau} - \epsilon_{\mu\mu}$). Recently, coherent neutrino-nucleus scattering has been observed for the first time by the COHERENT experiment [53], allowing for the derivation of competitive constraints on each of the diagonal parameters separately [38]. This is particularly relevant for ϵ_{ee}^{qV} and $\epsilon_{\tau\tau}^{qV}$ for which new 90% CL bounds are: $-0.045(0.037) < \epsilon_{ee}^{u(d)V} < 0.19(0.16)$ and $0.024(0.015) < \epsilon_{\tau\tau}^{u(d)V} < 0.30(0.27)$.

It is obvious that, for u -quark currents, the constraints from the LHC results are significantly stronger than those

from neutrino experiments, while those for the d -quark currents are more than competitive. At this stage, let us reexamine the NSI operators in totality. Since these, presumably, owe their origin to physics beyond the SM, the operators in eq.(1) ought to be written in terms of $SU(2)_L \otimes U(1)_Y$ invariant terms. For a pair of lepton doublets $L_{\alpha,\beta}$, the triplet combination would introduce terms of the form $(\bar{\nu}_\alpha \gamma_\mu P_L \ell_\beta) (\bar{d} \gamma^\mu P_L u)$ leading to extra contributions to well-measured meson decays (or, the decay of a τ to a meson). In the context of the LHC, on the other hand, this would lead to lepton nonuniversality in $pp \rightarrow \ell + \nu$ (exclusive or inclusive). Both sets of observables would lead to constraints much stronger than those discussed above. On the other hand, were we to consider a singlet structure, namely,

$$\bar{L}_\alpha \gamma_\mu L_\beta = \bar{\nu}_\alpha \gamma_\mu \nu_\beta + \bar{\ell}_\alpha \gamma_\mu \ell_\beta ,$$

clearly $\alpha \neq \beta$ would lead to $pp \rightarrow \ell_\alpha + \bar{\ell}_\beta$. Vetoing events with substantial missing energy (thereby suppressing the WW background) would lead to spectacular signals for $\epsilon_{\alpha\beta}$ being considered here. Even stronger bounds would emanate from lepton flavour changing decays of neutral mesons.

For $\alpha = \beta$, the charged lepton bounds are, understandably, weaker. However, even in this case, high-mass dilepton (e^\pm or μ^\pm) production constrains 4-fermi operators to a contact interaction scale of $\gtrsim 25$ TeV [54]. Translated to our language, this would imply $\epsilon_{ee}^{u,d}, \epsilon_{\mu\mu}^{u,d} \lesssim 5 \times 10^{-5}$. In principle, even stronger bounds can be obtained by considering asymmetries [55]. It would seem, thus, that $\epsilon_{\tau\tau}^{u,d}$ are the only Wilson coefficients (for first-generation quarks) that would have remained significantly unconstrained by either low-energy observables or LHC observables such as dilepton production. However, our analysis improves the situation dramatically, and far supersedes the COHERENT bounds [38]. Note, furthermore, that we

have not included the CMS data yet, which too does not show any excess in the monojet signal. However, with the CMS typically imposing softer requirements on both the leading jet and \cancel{E}_T , the reported exclusion [28] of σ_{BSM} is weaker than that in Ref. [54]. Once CMS reanalyses their data, the ensuing constraints can be combined with those reported here to yield significantly stronger bounds.

The narrative would change were we to consider suppressing operators involving the charged lepton by means of postulating multiple $SU(2)_L \otimes U(1)_Y$ invariant operators with carefully tuned WCs [56]. A different approach would be to postulate dimension-8 operators such as $[(\phi^* \bar{L}_\alpha) \gamma_\mu (\phi L)] (\bar{q} \gamma^\mu q)$ where ϕ is the SM Higgs doublet. In either case, charged-lepton 4-fermion operators do not exist, and the low-energy constraints are rendered very weak. Similarly, the simplest collider constraints are not operative either, and while more exotic signatures are suddenly possible, the corresponding cross sections are too small to be of any interest with the currently accumulated luminosity. However, as we have conclusively established in this article, even these scenarios (and any variants thereof) are already severely constrained by a simple final state such as a monojet with missing energy. And with the luminosity that the LHC is slated to deliver, continuing negative results would only strengthen the constraint to well beyond what even a next-generation neutrino experiment will be able to probe [14, 57–60]. This would indicate that the only role such facilities may play in this regard would be the confirmatory one.

DC acknowledges partial support from the European Unions Horizon 2020 research and innovation programme under Marie Skłodowska-Curie grant No 674896, and the R&D grant of the University of Delhi. KG is supported by the DST (India) under INSPIRE Faculty Award. SN acknowledges the hospitality of the Institute of Physics, Bhubaneswar during the initial phase of the work.

-
- [1] A. Pilaftsis and T. E. J. Underwood, Phys. Rev. **D72**, 113001 (2005), hep-ph/0506107.
- [2] D. Choudhury, N. Mahajan, S. Patra, and U. Sarkar, JCAP **1204**, 017 (2012), 1104.1851.
- [3] R. Barbieri and R. N. Mohapatra, Phys. Lett. **B218**, 225 (1989).
- [4] K. S. Babu and R. N. Mohapatra, Phys. Rev. Lett. **63**, 938 (1989).
- [5] D. Choudhury and U. Sarkar, Phys. Lett. **B235**, 113 (1990).
- [6] D. Choudhury and U. Sarkar, Phys. Rev. Lett. **68**, 2875 (1992).
- [7] J. R. Bhatt, B. R. Desai, E. Ma, G. Rajasekaran, and U. Sarkar, Phys. Lett. **B687**, 75 (2010), 0911.5012.
- [8] C. Wetterich, Nucl. Phys. **B897**, 111 (2015), 1408.0156.
- [9] N. Fornengo, M. Maltoni, R. Tomas, and J. Valle, Phys.Rev. **D65**, 013010 (2002), hep-ph/0108043.
- [10] P. Huber and J. Valle, Phys.Lett. **B523**, 151 (2001), hep-ph/0108193.
- [11] M. Gonzalez-Garcia and M. Maltoni, Phys.Rev. **D70**, 033010 (2004), hep-ph/0404085.
- [12] M. Gonzalez-Garcia, M. Maltoni, and J. Salvado, JHEP **1105**, 075 (2011), 1103.4365.
- [13] A. Esmaili, D. Gratieri, M. Guzzo, P. de Holanda, O. Peres, et al., Phys.Rev. **D89**, 113003 (2014), 1404.3608.
- [14] A. Chatterjee, P. Mehta, D. Choudhury, and R. Gandhi, Phys. Rev. **D93**, 093017 (2016), 1409.8472.
- [15] A. Chatterjee, R. Gandhi, and J. Singh, JHEP **1406**, 045 (2014), 1402.6265.
- [16] A. Datta, R. Gandhi, P. Mehta, and S. U. Sankar, Physics Letters B **597**, 356 (2004).
- [17] A. Esmaili, O. Peres, and Z. Tabrizi (2014), 1409.3502.
- [18] A. Esmaili, F. Halzen, and O. Peres, JCAP **1211**, 041 (2012), 1206.6903.
- [19] A. Esmaili, F. Halzen, and O. Peres, JCAP **1307**, 048 (2013), 1303.3294.
- [20] A. Esmaili and A. Y. Smirnov, JHEP **1312**, 014 (2013),

- 1307.6824.
- [21] S. Davidson and V. Sanz, Phys. Rev. **D84**, 113011 (2011), 1108.5320.
- [22] A. Friedland, M. L. Graesser, I. M. Shoemaker, and L. Vecchi, Phys. Lett. **B714**, 267 (2012), 1111.5331.
- [23] S. Davidson and V. Sanz, J. Phys. Conf. Ser. **408**, 012033 (2013), 1110.1558.
- [24] D. Buarque Franzosi, M. T. Frandsen, and I. M. Shoemaker, Phys. Rev. **D93**, 095001 (2016), 1507.07574.
- [25] Tech. Rep. ATLAS-CONF-2017-060, CERN, Geneva (2017), URL <https://cds.cern.ch/record/2273876>.
- [26] M. Aaboud et al. (ATLAS) (2017), 1711.03301.
- [27] A. M. Sirunyan et al. (CMS), JHEP **07**, 014 (2017), 1703.01651.
- [28] A. M. Sirunyan et al. (CMS) (2017), 1712.02345.
- [29] A. Alloul, N. D. Christensen, C. Degrande, C. Duhr, and B. Fuks, Comput. Phys. Commun. **185**, 2250 (2014), 1310.1921.
- [30] N. D. Christensen and C. Duhr, Comput. Phys. Commun. **180**, 1614 (2009), 0806.4194.
- [31] J. Alwall, R. Frederix, S. Frixione, V. Hirschi, F. Maltoni, O. Mattelaer, H. S. Shao, T. Stelzer, P. Torrielli, and M. Zaro, JHEP **07**, 079 (2014), 1405.0301.
- [32] R. D. Ball et al., Nucl. Phys. **B867**, 244 (2013), 1207.1303.
- [33] T. Sjostrand, S. Mrenna, and P. Z. Skands, JHEP **05**, 026 (2006), hep-ph/0603175.
- [34] M. Cacciari, G. P. Salam, and G. Soyez, Eur. Phys. J. **C72**, 1896 (2012), 1111.6097.
- [35] M. Cacciari, G. P. Salam, and G. Soyez, JHEP **04**, 063 (2008), 0802.1189.
- [36] M. Aaboud et al. (ATLAS), Phys. Rev. **D94**, 032005 (2016), 1604.07773.
- [37] M. C. Gonzalez-Garcia and M. Maltoni, JHEP **09**, 152 (2013), 1307.3092.
- [38] P. Coloma, M. C. Gonzalez-Garcia, M. Maltoni, and T. Schwetz, Phys. Rev. **D96**, 115007 (2017), 1708.02899.
- [39] R. Wendell et al. (Super-Kamiokande), Phys. Rev. **D81**, 092004 (2010), 1002.3471.
- [40] P. Adamson et al. (MINOS), Phys. Rev. Lett. **110**, 251801 (2013), 1304.6335.
- [41] P. Adamson et al. (MINOS), Phys. Rev. Lett. **110**, 171801 (2013), 1301.4581.
- [42] K. Abe et al. (T2K), Phys. Rev. Lett. **112**, 061802 (2014), 1311.4750.
- [43] K. Abe et al. (T2K), Phys. Rev. Lett. **107**, 041801 (2011), 1106.2822.
- [44] A. Gando et al. (KamLAND), Phys. Rev. **D83**, 052002 (2011), 1009.4771.
- [45] M. Apollonio et al. (CHOOZ), Phys. Lett. **B466**, 415 (1999), hep-ex/9907037.
- [46] A. Piepke (Palo Verde), Prog. Part. Nucl. Phys. **48**, 113 (2002), [113(2002)].
- [47] F. P. An et al. (Daya Bay), Chin. Phys. **C37**, 011001 (2013), 1210.6327.
- [48] J. K. Ahn et al. (RENO), Phys. Rev. Lett. **108**, 191802 (2012), 1204.0626.
- [49] F. J. Escrivuela, M. Tortola, J. W. F. Valle, and O. G. Miranda, Phys. Rev. **D83**, 093002 (2011), 1103.1366.
- [50] G. P. Zeller et al. (NuTeV), Phys. Rev. Lett. **88**, 091802 (2002), [Erratum: Phys. Rev. Lett.90,239902(2003)], hep-ex/0110059.
- [51] J. V. Allaby et al. (CHARM), Z. Phys. **C36**, 611 (1987).
- [52] A. Blondel et al., Z. Phys. **C45**, 361 (1990).
- [53] D. Akimov et al. (COHERENT), Science **357**, 1123 (2017), 1708.01294.
- [54] M. Aaboud et al. (ATLAS), JHEP **10**, 182 (2017), 1707.02424.
- [55] D. Choudhury, R. M. Godbole, and G. Polesello, JHEP **08**, 004 (2002), hep-ph/0207248.
- [56] C. Biggio, M. Blennow, and E. Fernandez-Martinez, JHEP **08**, 090 (2009), 0907.0097.
- [57] S. Choubey, A. Ghosh, T. Ohlsson, and D. Tiwari, JHEP **12**, 126 (2015), 1507.02211.
- [58] S. Choubey and T. Ohlsson, Phys. Lett. **B739**, 357 (2014), 1410.0410.
- [59] S. Fukasawa, M. Ghosh, and O. Yasuda, Phys. Rev. **D95**, 055005 (2017), 1611.06141.
- [60] T. Ohlsson, Rept. Prog. Phys. **76**, 044201 (2013), 1209.2710.